

## MICRODOSIMETRY

Nota di STEFANO AGOSTEO (\*)

(Adunanza del 24 marzo 2022)

SUNTO. – L'applicazione della microdosimetria per la stima della qualità dei campi di adroterapia oncologica ha suscitato un crescente interesse negli ultimi vent'anni. Il rivelatore di riferimento nella microdosimetria è il "tissue-equivalent proportional counter (TEPC)" o contatore di Rossi. Il Laboratorio di Misure Nucleari del Politecnico di Milano collabora da decenni con i Laboratori Nazionali di Legnaro dell'INFN per il progetto e la costruzione di nuovi microdosimetri. In questo lavoro sono discusse le caratteristiche principali di una TEPC a confinamento di valanga, in grado di simulare siti fino a 25 nm, e un telecopio al silicio. Nell'Introduzione sono anche definite le principali grandezze dosimetriche e microdosimetriche per completezza.

\*\*\*

ABSTRACT. – The interest in the application of microdosimetry for assessing the radiation quality of hadrontherapy fields has grown in the last two decades. The reference detector for microdosimetry is the tissue-equivalent proportional counter (TEPC). Novel types of microdosimeters have been developed by the Nuclear Measurement Laboratory of the Politecnico di Milano in collaboration with the INFN National Legnaro Laboratories. This work describes the main features of an avalanche confinement TEPC, capable of simulating sites down to 25 nm and a silicon telescope detector. The main dosimetric and microdosimetric quantities are also given and discussed in the Introduction for the sake of clarity.

---

(\*) Dipartimento di Energia, Sezione di Ingegneria Nucleare – CeSNEF, Politecnico di Milano, Italy. E-mail: stefano.agosteo@polimi.it

## 1. INTRODUCTION

The ICRP Publication n.103 [1] states that “the fluctuations of energy deposited in individual cells and sub cellular structures and the microscopic tracks of charged particles are the subject of *microdosimetry*”. The experimental microdosimetry [2] is defined as “the study and the interpretation of single-event energy deposition spectra measured using low pressure proportional counters to simulate microscopic sites of tissue”.

Some dosimetric quantities are defined in the following for the sake of completeness.

The *restricted LET* (Linear Energy Transfer) is defined for charged particles (*e.g.*, electrons, protons, ions, etc.) as:

(1)

where  $dE$  is the mean energy deposited along the particle track length  $dx$ , only by accounting for collisions leading to transfers of energy lower than  $\Delta$  (in eV). When  $\Delta = \infty$  (*unrestricted LET*), all energy losses are accounted for. Muscular (soft) tissue is the material in which these energy transfers (induced by atomic and molecular ionization and excitation) occur. Energy losses referring to the restricted *LET* can be considered included in a cylinder centered on the particle track, whose radius is equal to the range in tissue of electrons  $\Delta$  in energy. When considering the *unrestricted LET*, energy is assumed to be deposited locally along the track length, since any information about its radial deposition cannot be inferred. The *LET* does not account for the stochastic and discrete behavior of energy deposition of radiation. For this reason and in such conditions, the so-called continuous slowing-down approximation (c.s.d.a.) holds.

The ICRU Publication n. 51 [3] defines the energy imparted to matter in a volume through the *radiant energy*  $R$ , in turn defined as the emitted, transferred or received energy of a particle (rest energy excluded). The unit of  $R$  is the joule (J). The energy imparted by ionizing radiation to matter is defined as:

$$\varepsilon = R_{in} - R_{out} + \sum Q \quad (2)$$

where:

- $R_{in}$  is the radiant energy impinging on the volume, *i.e.*, the sum of the energies of all the charged and uncharged ionizing particles (by excluding their rest energy) entering the volume;
- $R_{out}$  is the radiant energy emerging from the volume, *i.e.*, the sum of the energies (rest energy excluded) of all particles leaving the volume;
- $\sum Q$  is the sum of all the rest energy variations of nuclei and elementary particles in each interaction occurring in the considered volume.

The *absorbed dose*  $D$  is defined as the ratio:

$$D = \frac{d\bar{\varepsilon}}{dm} \quad (3)$$

where  $d\bar{\varepsilon}$  is the *mean* energy imparted by ionizing radiation to matter  $dm$  in mass. The absorbed dose unit is the gray (Gy).  $1 \text{ Gy} = 1 \text{ J kg}^{-1}$ .

It should be stressed that:

- the absorbed dose is a non-stochastic quantity;
- it cannot express the radiation damage, *i.e.*, it is not linked directly to biological effects of radiation. Further information (and quantities) is required for this purpose, as the energy and the particle type, their linear energy transfer (*LET*) and, more specifically, their track structure. The probability density of some microdosimetric quantities is a piece of information more linked to biological effects, but it might not be sufficient;
- it is simple to define. It should be noted that the absorbed dose is the quantity prescribed to patients in radiation therapy;
- it is easily measurable at a low-cost.

It should be noted that the extent of the mass  $dm$  is not specified. The extent of the volume including  $dm$  should assure that the *mean value* of imparted energy could be defined. In other words, the number of events occurring in that volume should be sufficiently high. Moreover, energy should be deposited homogeneously inside that volume. For very

small volumes, of the order of cellular dimensions (a few  $\mu\text{m}$ ) or of DNA dimensions (about 2 nm in thickness), this concept has no meaning, because a single event (or even no event) can occur. Stochastic quantities should be used, like the ones defined for microdosimetry.

It should be observed that the ratio  $\varepsilon/m$  fluctuates strongly when the value of  $m$  is reduced further, because of the discrete trend of energy transfer events. For very low mass values, the ratio  $\varepsilon/m$  will be equal to zero in most of cases, but, when the energy transfer occurs within the considered infinitesimal site, it will gain very high values which can be orders of magnitude higher than that of the absorbed dose. Fluctuations depend on energy deposition through discrete events promoted by charged particles and therefore the local energy density in very small masses depends on the number of particles transferring their energy in the considered infinitesimal volume. The absorbed dose is a macroscopic quantity, such as temperature or pressure. On the other hand, it should be stressed that the biological and chemical effects of radiation are due to the high  $\varepsilon/m$  values which are achieved inside infinitesimal volumes. The high  $\varepsilon/m$  values at the dimensions where this ratio acquires a stochastic behaviour correspond to macroscopic values of absorbed dose which would be responsible for killing a big animal.

A significant quantity for expressing biological effects of radiation is the *relative biological effectiveness* (*RBE*), which accounts for the response to different radiation fields in a cell culture:

$$RBE = \frac{D_{ref}}{D} \quad (4)$$

where  $D$  is the absorbed dose required to produce a given effect (*e.g.*, a given survival fraction) on the irradiated system with a given radiation field and  $D_{ref}$  is the absorbed dose from the reference radiation field producing the same biological effect in the same cell system. Generally, although there is no international agreement about this issue, the reference radiation field is constituted by 150 kV X rays or by gamma rays from  $^{60}\text{Co}$  decay. The *RBE* depends on the absorbed dose, cell type and biological end-point [4]. The *RBE* dependence on the LET was observed in many cell systems, but this is not a univocal relation, since different particles may show the same LET value, but a different track structure leading to a different effect.

Radiation damage at the DNA level is closely linked to the particle track structure. The unrestricted LET does not give any information about the track structure, which also consists of delta-ray electrons.

The microdosimetric quantities are defined in the ICRU publication no. 36 [5]. The fundamental stochastic quantities are the specific energy  $z$  and the lineal energy  $y$ , defined as:

$$z = \frac{\varepsilon}{m} \quad (5)$$

$$y = \frac{\varepsilon}{\bar{\ell}} \quad (6)$$

where  $\varepsilon$  is the imparted energy (which is a stochastic quantity),  $m$  the mass contained in a volume (site) and  $\bar{\ell}$  the mean chord length in a volume. Lineal energy is defined for a single energy deposition event. The unit of the specific and the lineal energy is the gray (Gy) and the keV  $\mu\text{m}^{-1}$ , respectively. Only the lineal energy will be accounted for in the following, since usually the radiation quality is assessed in terms of it.

The probability density  $f(y)$  is also referred as lineal energy distribution or frequency distribution:  $\int_{y_1}^{y_2} f(y)dy$  gives the fraction of events in a given interval from  $y_1$  to  $y_2$ . The dose distribution  $d(y)$  is usually referred as *microdosimetric distribution*:  $\int_{y_1}^{y_2} d(y)dy$  expresses the fraction of absorbed dose in a given interval from  $y_1$  to  $y_2$ . It should be remembered that both the distributions refer to a single event only. The expectation values of the lineal energy and the dose distribution (frequency-mean lineal energy and dose-mean lineal energy, respectively) are:

$$\bar{y}_F = \int_0^{\infty} yf(y)dy \quad (7)$$

$$\bar{y}_D = \int_0^{\infty} yd(y)dy \quad (8)$$

$d(y)$  and  $f(y)$  are related by the following equation:

$$d(y) = \frac{yf(y)}{\bar{y}_F} \quad (9)$$

and therefore:

$$\bar{y}_D = \frac{1}{\bar{y}_F} \int_0^\infty y^2 f(y) dy \quad (10)$$

For gas detectors, such as tissue-equivalent proportional counters (TEPCs), a tissue site of micrometric dimensions can be simulated by a macroscopic cavity filled with a low-pressure gas, if the energy loss of charged particles traversing the cavity is the same as in a tissue site traversed with an equivalent trajectory. For a tissue sphere  $d_t$  in diameter and a gas sphere  $d_g = k d_t$  in diameter, the condition is:

$$\Delta E_t = \left(\frac{S}{\rho}\right)_t \rho_t d_t = \left(\frac{S}{\rho}\right)_g \rho_g d_g = \Delta E_g \quad (11)$$

where  $\Delta E_t$  and  $\Delta E_g$  are the mean energy losses of charged particles in tissue and in the gas, respectively,  $(S/\rho)_t$  and  $(S/\rho)_g$  are the mass stopping powers of charged particles in tissue and in the gas, respectively and  $\rho_t$  and  $\rho_g$  the tissue and gas density. The above equation has been written for a particle traversing the site along its diameter, but it holds for any trajectory traversing the site. If the chemical composition of gas and tissue are the same (practically, if the gas is tissue-equivalent) and if the stopping powers are independent of density:

$$\rho_g = \frac{\rho_t}{k} \quad (12)$$

The site size can be modified by adjusting the gas pressure in a TEPC of given dimensions.

The microdosimetric distributions contain most of the information about the radiation quality of a therapeutic beam. *Fig. 1* shows a set of microdosimetric distributions measured at different positions along the depth-dose profile of the spread-out Bragg peak (SOBP) from 62 MeV protons delivered at the INFN-CATANA facility (Istituto Nazionale di Fisica Nucleare, INFN; Laboratori Nazionali del Sud, LNS, Catania, Italy) for treating eye tumours. These measurements were performed with an avalanche-confinement TEPC (Section 3) simulating a 300 nm site. The distributions shift towards higher lineal energy values with increasing depth and, therefore, proton *LET*. This shift indicates a change in the radiation quality since the distributions are seated on higher lineal energy values, thus signalling an *LET* increase of the radiation field.

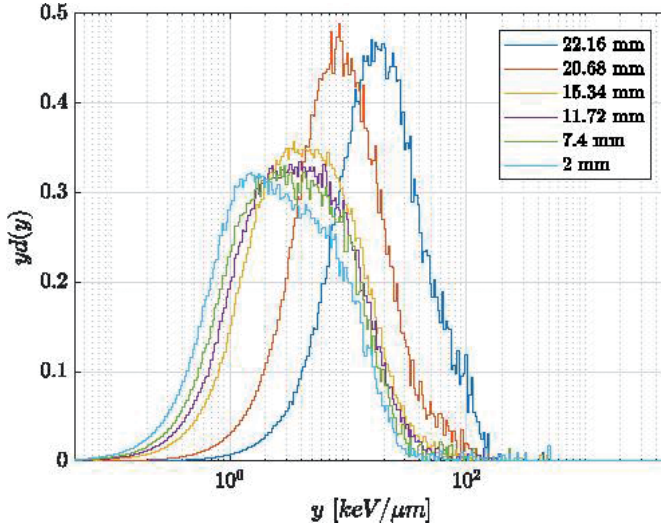


Fig. 1. Microdosimetric distributions for different positions across the CATANA proton SOBPs measured with an avalanche-confinement TEPC in a simulated 300 nm site.

## 2. RADIATION QUALITY

The interest in the application of microdosimetry for assessing the radiation quality of hadrontherapy fields has grown in the last two decades. Radiation quality is closely related to the linear energy transfer ( $LET$ ), which, in the case of hadron beams varies across the depth-dose distribution of the therapeutic beam, resulting in a different biological and clinical response.

As already mentioned, microdosimetry is based on stochastic quantities which express the fluctuations of energy deposition in micrometric and sub-micrometric structures, while the  $LET$  is a non-stochastic quantity giving the mean energy transferred in an infinitesimal part of the particle path.

The dose-mean lineal energy  $\bar{y}_D$  is one of the microdosimetric quantities which can be employed for expressing the radiation quality. Fig. 2 shows the  $\bar{y}_D$  at different positions along the depth-dose profile of the CATANA proton SOBPs measured with the same avalanche confinement TEPC for different simulated site sizes. The  $\bar{y}_D$  trend signals

clearly the radiation quality increase with depth. In other words, a higher  $\bar{y}_D$  value is related to a higher radiation quality, at least below the values for which the overkilling effect becomes predominant.

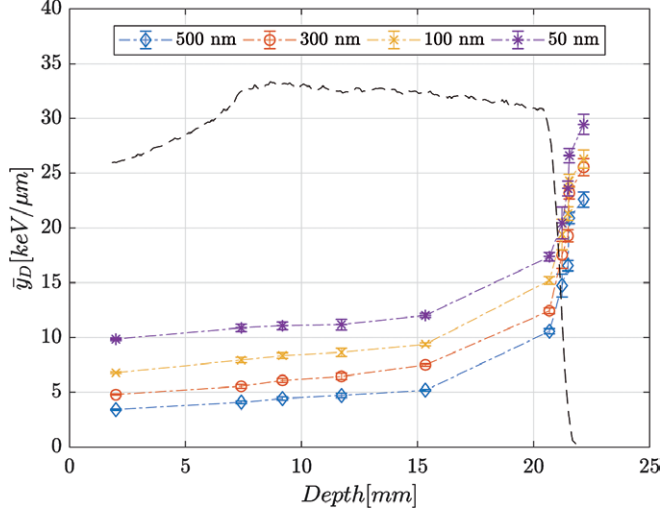


Fig. 2. Dose-mean lineal energies and uncertainty bars for different simulated site sizes and for different positions across the spread-out Bragg peak (SOBP). The dashed line indicates the depth-dose curve of the proton SOBP.

Another quantity employed for expressing the radiation quality of therapeutic beams is the microdosimetric  $RBE_\mu$  [6]. It can be assessed by folding the dose probability density  $d(y)$  with an RBE-weighting function  $r(y)$ :

$$RBE_\mu = \int_0^{\infty} r(y)d(y)dy \quad (13)$$

It should be stressed that this is not an estimate of the RBE. It should also be remembered that RBE is not a unique and not a physical quantity and therefore it cannot be measured directly with an instrument. RBE is referring to a particular biological endpoint (such as, *e.g.* a particular value of clonogenic survival probability) and can be assessed only through radiobiological experiments by irradiating cell cultures. It depends strongly on the type of irradiated cells, the dose, the physiological conditions of the sample, etc. The  $RBE_m$  is a param-

ter which can only be useful for expressing the radiation quality. It is assessed through the weighting function  $r(y)$  which refer to radiobiological effects induced in specified samples under specified irradiation conditions and to microdosimetric spectra measured inside simulated sites of specified dimensions. The  $r(y)$  function was first derived by Loncol *et al.* [7] from RBE values ( $^{60}\text{Co}$  as reference radiation) for early effects (intestinal crypt regeneration) in mice at 8 Gy and from microdosimetric spectra measured in 2  $\mu\text{m}$  simulated site for photon, proton and fast neutron fields [8]. Another weighting function  $r(y)$  was proposed more recently by [9] from RBE literature data for the 10% survival of V79 Chinese hamster lung fibroblasts. For calculating this weighting function, radiation transport was simulated with a Monte-Carlo code for a wide set of ions from protons up to  $^{238}\text{U}$ , thus completing the data set by Loncol *et al.* [7].

### 3. DETECTORS DEVELOPED AT THE POLITECNICO DI MILANO

Among the variety of detectors employed in microdosimetry (TEPCs, silicon detectors, gas-electron multipliers, diamond detectors) only the ones developed at the Laboratory of Nuclear Measurements of the Politecnico di Milano in collaboration with the INFN-Legnaro National Laboratories (Legnaro, Italy) are discussed in this Section.

An avalanche-confinement TEPC operating at a nanometric level was designed and constructed by Cesari *et al.* [10] and upgraded by Bortot *et al.* [11]. The design of the new TEPC includes a thinner-walled chamber, which allows measuring low-energy (and high-LET) hadron beams, a removable internal alpha source and a very compact solid-state detector (SSD) inserted into the sensitive zone for energy calibration. The TEPC was designed for simulating sites in the range from 0.3  $\mu\text{m}$  down to 25 nm.

The cylindrical sensitive volume of the detector (13 mm in diameter and length) houses three electrodes biased independently: a central anode wire (graphite, 1 mm in diameter), a cylindrical cathode shell (conductive plastic A-150 type, 13 mm in internal diameter and 1 mm in thickness) and a helix (gold-plated tungsten, 100  $\mu\text{m}$  in diameter) made of 19 coils, 6 mm in inner diameter. This helix surrounds the anode wire and subdivides the sensitive volume into an external drift zone and an internal multiplication region (*Fig. 3*).

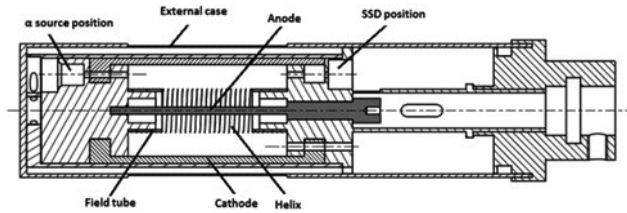


Fig. 3. Cross-sectional view of the avalanche-confinement TEPC. The locations of the calibration alpha source and the solid state detector (SSD) are indicated.

Two field tubes (stainless steel, 6 mm in diameter) are employed both for sustaining the helix and for defining the sensitive volume, which is a right cylinder 13 mm both in diameter and length, thus avoiding any distortion of the electric field, while two insulating Rexolite caps enclose the chamber. An orifice was drilled into the basis cap to allow a gas flow. Two aligned holes were also drilled into the Rexolite caps in order to contain a thick removable Cm-244 alpha source, sealed by a mylar layer, and a miniaturized solid-state detector (SSD). This configuration allows calibrating the TEPC by also varying *i*) the simulated site size and *ii*) the polarization of the three electrodes. It guarantees that only signals due to alpha particles with a straight path inside the sensitive volume, *i.e.* the drift region, are collected [12]. Particles ionizing the gas inside the multiplication region affect slightly the microdosimetric distribution, since its volume is about 20% of the whole sensitive region and charge multiplication of particles ionizing the gas inside the confining helix is lower. This avalanche-confinement TEPC showed to be capable of measuring in the range 0.3  $\mu\text{m}$  - 25 nm when irradiated with carbon [11], helium [13] ions and protons down to 35 nm [14]. A characterization of 195.2 MeV per nucleon carbon ions irradiating a PMMA phantom was carried out at the CNAO by simulating site sizes in the range 25-500 nm [15]. The spectra turned out to be influenced by secondary delta-ray electrons when decreasing the site size for the same phantom depth. A shift towards high lineal energies was observed while decreasing the site size at depths proximal to the Bragg peak. At distal depths, the edge of the spectrum was found to be independent of the simulated site size. The same independence was also observed for helium ions, the CATANA clinical proton beam and when irradiating the detector with a  $^{137}\text{Cs}$  source.

It should be stressed that the geometry of the sensitive volume, defined by the hollow-cylindrical drift region external to the helix,

together with the presence of the fairly thick central anode lead to calculate the mean chord length depending on the irradiation geometry (which is a parallel beam normal to the anode for charged hadron beams) with Monte Carlo simulations or analytically [16].

The micrometric sensitive volumes (SV) which can be fabricated for silicon detectors have led to these devices being studied as microdosimeters. They can be applied for assessing single event effects in electronic instrumentation exposed to complex fields around high-energy accelerators or in space missions. When coupled to tissue-equivalent converters or inserted in tissue-equivalent phantoms, they can be used for measuring the quality of radiation therapy beams. Detailed reviews of silicon microdosimetry were given in [17-19].

A monolithic silicon telescope was proposed by Agosteo *et al.*, [20] as a microdosimeter, basing on a detector designed by Tudisco *et al.* (1996) and fabricated by ST Microelectronics (Catania, Italy). The first model consisted by a single  $\Delta E$  element 2  $\mu\text{m}$  in thickness and a 500  $\mu\text{m}$  thick residual energy E-stage (Fig. 4). The  $\Delta E$  and the E elements are separated by a deep-implanted p+ electrode which acts a watershed for charge collection, thus minimizing the field-funneling effect. The thin  $\Delta E$  element acts as a microdosimeter. The SV sensitive area is about 1  $\text{mm}^2$ . This single-stage configuration showed some limitations for an isotropic irradiation field since the length of a tilted particle track can be millimetric. In any case, this microdosimeter showed a good agreement with a mini-TEPC when irradiated with parallel clinical beams.

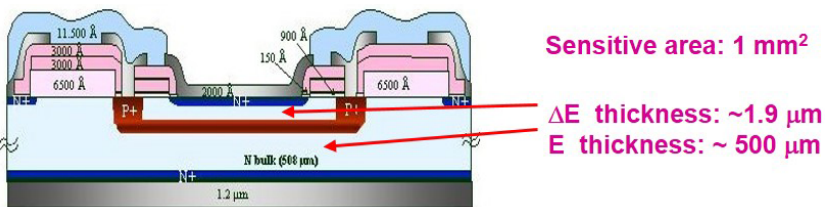


Fig. 4 The single- $\Delta E$  monolithic silicon telescope. The  $\Delta E$  and the residual energy elements are indicated.

The pixelated silicon microdosimeter proposed by Agosteo *et al.* [21] (Fig. 5) minimizes the effect mentioned above. It consists of a matrix of cylindrical  $\Delta E$  elements (about 2  $\mu\text{m}$  in thickness) and a single resid-

ual-energy E stage (500  $\mu\text{m}$  thick). The nominal diameter of the  $\Delta E$  elements is about 9  $\mu\text{m}$  and the width of the pitch separating the elements is about 41  $\mu\text{m}$ . More than 7000 pixels are connected in parallel to give an effective sensitive area of about 0.5  $\text{mm}^2$ . A guard ring hinders charge collection outside the SV. The minimum detectable energy is limited to about 20 keV (corresponding to about 7-8 keV  $\mu\text{m}^{-1}$  in lineal energy) by the electronic noise. Therefore, the applicability of this silicon microdosimeter is limited to high LET particles. The  $\Delta E$  stage acts as a microdosimeter and the E stage plays a fundamental role for assessing the full energy of the interacting particles, thus allowing an LET-dependent correction for tissue-equivalence to be performed event-by-event. An example referring to proton irradiations is given in the following.

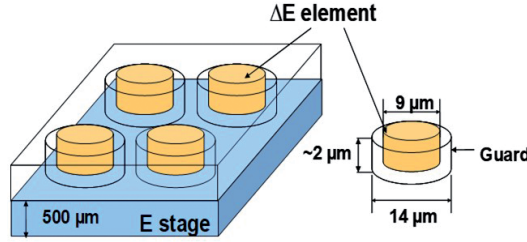


Fig. 5. The pixelated silicon microdosimeter. Only a few elements of the matrix of about 7,000 cylindrical  $\Delta E$  stages (about 2  $\mu\text{m}$  in thickness) are sketched over the single residual-energy E stage (500  $\mu\text{m}$  thick).

The event-by-event tissue-equivalence correction can be adopted when protons stop completely in the E stage, thus allowing to measure their impinging energy. This complete energy deposition in the silicon telescope occurs for protons up to about 10 MeV, whose range in silicon corresponds to the thickness of the E-stage (500  $\mu\text{m}$ ). In the energy range below 10 MeV the ratio  $R(E_p)$  of the stopping power of protons in tissue  $S^{Tissue}(E_p)$  to that in silicon  $S^{Si}(E_p)$  shows a fairly high variation. In this case, the energy  $E_{\Delta E}^{Si}$  (energy deposited in the silicon  $\Delta E$  stage) can be corrected for the energy-dependent ratio  $R(E_p)$ :

$$E_{\Delta E}^{Tissue}(E_p) = E_{\Delta E}^{Si}(E_p) \cdot \frac{S^{Tissue}(E_p)}{S^{Si}(E_p)} \quad (14)$$

where  $E_p$  is calculated by summing the energy deposited in both detector stages and  $E_{AE}^{Tissue}(E_p)$  is the corresponding energy which would be deposited in tissue.

When protons cross completely the E stage (*i.e.*, above about 10 MeV), no information about the energy  $E_p$  of the impinging protons is available. For these energies, the ratio  $R(E_p)$  ranges from 0.556 to 0.585 and the use of an average factor  $\zeta$  is acceptable. Therefore, the energy  $E_{\Delta E}^{Si}$ , measured with the silicon  $\Delta E$  stage, is scaled with a constant factor  $\zeta$  equal to 0.574, obtained by averaging over the energy interval of interest the energy-dependent ratio  $R(E_p)$ .

When comparing the microdosimetric spectra from a detector with a sensitive volume with a different geometry (*e.g.*, a TEPC) a shape-equivalence correction has to be carried out. As described in details by Agosteo *et al.* [21] for the silicon telescope described herein, this shape-equivalence correction consists in calculating the lineal energy  $y$  by dividing the imparted energy  $E_{\Delta E}^{Tissue}$  by an equivalent mean chord length  $\ell_{eq}$ , equal to the product of the actual mean chord length  $\ell$  times a coefficient  $\eta$  (equal to 0.533). This coefficient was derived through parametric criteria discussed by Kellerer [22]. The coefficient  $\eta$  depends only on the geometry of the sensitive volume of the two detectors.

The microdosimetric spectra acquired at the CATANA facility at four position across the distal fall-off of the 62 MeV proton Bragg peak are shown in *Fig. 6* [23]. These spectra are compared with the ones acquired at the same positions with a reference TEPC.

The configuration of this telescope detector also allows to discriminate different types of charged particles interacting with the  $\Delta E$ -E elements through the so-called “scatter-plot”, showing the energy deposited in the  $\Delta E$  element against that deposited in the E element. *Fig. 7* shows the scatter plot acquired at 8 mm in depth of a PMMA phantom irradiated with 62 MeV per nucleon carbon ions at the LNS. This depth is higher than the range (the depth at which charged particles of a given energy stop completely) of the primary carbon ion beam and therefore only light ions from projectile fragmentation are detected.

Colautti *et al.* [24] compared the response of four detectors (a mini-TEPC, a silicon telescope, a GEM and a diamond microdosimeter) irradiated with a beam of 62 MeV per nucleon carbon ions at the INFN-LNS in Catania (Italy). The acquired microdosimetric spectra showed significantly different shapes, as expected, since the detector SVs were different together with the properties of their constituting

materials. Nevertheless, a better agreement was found for the the  $\bar{y}_D$  values at the measured depths across the Bragg peak in a PMMA phantom. A similar trend was observed in [25], where the response of a mini-TEPC and a silicon telescope microdosimeter were compared for the therapeutic active scanning beam at the CNAO.

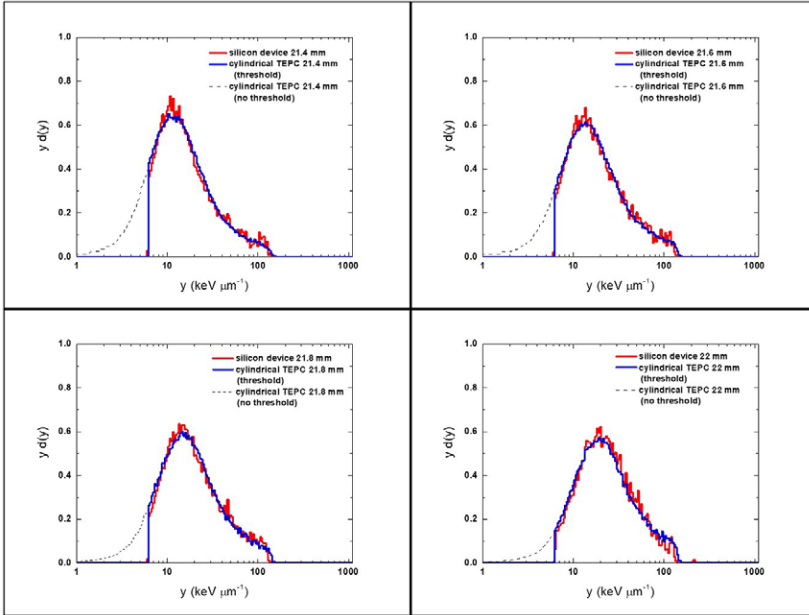


Fig. 6. Comparison between the lineal energy spectra obtained with the silicon telescope (red line) and those obtained with the reference TEPC (solid blue line) truncated at a value corresponding to the energy threshold of the silicon-based system ( $6 \text{ keV } \mu\text{m}^{-1}$ ). The non-normalized complete microdosimetric spectra measured by the TEPC are also shown (dashed blue line).

Bianchi *et al.* [26] compared the microdosimetric spectra from the mini-TEPC and a silicon telescope at various depths across the Bragg peak from the 62 MeV proton beam at the INFN-LNS CATANA facility. Again, the shape of the spectra showed some deviations even after the linear extrapolation of the silicon detector spectra down to  $0.01 \text{ keV } \mu\text{m}^{-1}$ . These discrepancies were attributed to the different chord length distribution and to the presence of wall effects in the mini-TEPC. In particular, the lineal energy distribution

was found to be wider especially at low  $y$ -values. This was due to a higher contribution of  $\delta$ -rays from the TEPC wall. In this case, the different shape of the microdosimetric spectra led to overestimate the  $\bar{y}_D$  values from the silicon device. However, the trend of the  $\bar{y}_D$  values against the depth of the Bragg peak was in a satisfactory agreement with the TEPC one. Therefore, a scaling factor was applied, resulting in a sort of a  $\bar{y}_D$ -calibration of the silicon microdosimeter.

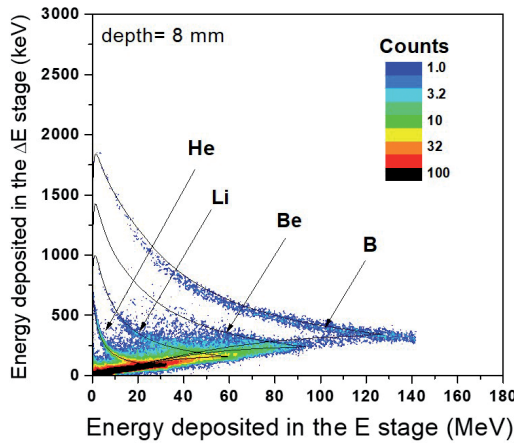


Fig. 7. Scatter plot of the energy deposited in the  $\Delta E$  element against that deposited in the E element acquired at 8 mm in depth of a PMMA phantom irradiated with 62 MeV per nucleon carbon ions at the LNS. At this depth only light ions from projectile fragmentation are present.

#### 4. CONCLUSIONS

Microdosimetry has been employed in the last decade for assessing the radiation quality of hadrontherapy fields, giving very useful pieces of information. Still the reference detector for microdosimetry is the tissue-equivalent proportional counter (TEPC), but new devices are being tested for this purpose.

As far as the silicon telescope detectors are concerned, some comparisons were carried out recently. It turned out that silicon telescope should be always compared with a reference TEPC before using them routinely in a given hadrontherapy field.

## BIBLIOGRAPHY

1. International Commission on Radiological Protection. The 2007 recommendations of the International Commission on Radiological Protection. ICRP Publication n. 103. Elsevier, 2007.
2. Waker, A.J., Principals of experimental microdosimetry, Radiation Protection Dosimetry, 1995: 61: 297-308.
3. International Commission on Radiation Units and Measurements. Quantities and units in radiation protection dosimetry. ICRU Report 51. ICRU, Bethesda, Maryland, 1993.
4. Nikjoo, H., Lindborg, L., RBE of low energy electrons and photons topical review. Phys.Med. Biol., 2010: 55: 65-109.
5. International Commission on Radiation Units and Measurements. Microdosimetry. ICRU Report 36. ICRU, Bethesda, Maryland, 1983.
6. De Nardo, L., Moro, D., Colautti, P., Conte, V., Tornielli, G., Cuttone, G., b. Microdosimetric investigation at the therapeutic proton beam facility of CATANA, Radiat. Prot. Dosim., 2004: 110: 681-686.
7. Loncol, T., Cosgrove, V., Denis, J.M., Gueulette, J., Mazal, A., Menzel, H.G., Pihet, P., Sabattier, R., Radiobiological effectiveness of radiation beams with broad LET spectra: microdosimetric analysis using biological weighting functions. Radiat. Prot. Dosim., 1994: 52: 347-352.
8. Colautti, P., Magrin, G., Palmans, H., Cortés-Giraldo, M.A., Conte, V., Characterizing Radiation Effectiveness in Ion-Beam Therapy Part II: Microdosimetric Detectors, Front. Phys., 2020, 8:550458.
9. Parisi, A., Sato, T., Matsuya, Y., Kase, Y., Magrin, G., Verona, C., Tran, L., Rosenfeld, A., Bianchi, A., Olko, P., Struelens, L., Vanhavere, F., Development of a new microdosimetric biological weighting function for the RBE<sub>10</sub> assessment in case of the V79 cell line exposed to ions from <sup>1</sup>H to <sup>238</sup>U, Phys. Med. Biol., 2020: 65: 235010.
10. Cesari, V., Colautti, P., Magrin, G., De Nardo, L., Baek, W.Y., Grosswendt, B., Alkaa, A., Khamphan, C., Ségur, P., Tornielli, G., Nanodosimetric measurements with an avalanche confinement TEPC. Radiat. Prot. Dosim., 2002: 99: 337-342.
11. Bortot, D., Pola, A., Agosteo, S., Pasquato, S., Mazzucconi, D., Fazzi, A., Colautti, P., Conte, V., A novel avalanche-confinement TEPC for microdosimetry at nanometric level. Radiation Measurements, 2017: 103: 1-12.
12. Bortot, D., Pola, A., Agosteo, S., Pasquato, S., Introini, M.V., Colautti, P., Conte, V., A miniaturized alpha spectrometer for the calibration of an avalanche-confinement TEPC. Radiation Measurements, 2017: 106: 531-537.
13. Mazzucconi, D., Bortot, D., Agosteo, S., Pola, A., Pasquato, S., Fazzi, A., Colautti, P., Conte, V., Petringa, G., Amico, A., Cirrone, G.A.P., Microdosimetry at nanometric scale with an avalanche-confinement TEPC: response against a helium ion beam. Radiation Protection Dosimetry, 2019: 183: 177-181.
14. Mazzucconi, D., Bortot, D., Pola, A., Fazzi, A., Colautti, P., Conte, V., Petringa, G., Cirrone, G.A.P., Agosteo, S., Nano-microdosimetric investigation at the therapeutic proton irradiation line of CATANA. Radiation Measurements, 2019: 123: 26-33.

15. Bortot, D., Mazzucconi, D., Pola, A., Fazzi, A., Pullia, M., Savazzi, S., Colautti, P., Conte, V., Agosteo, S., A nano-microdosimetric characterization of a therapeutic carbon ion beam at CNAO. *Radiation Physics and Chemistry*, 2020: 170: 108674.
16. Mazzucconi, D., Bortot, D., Pola, A., Agosteo, S., Pasquato, S., Fazzi, A., Colautti, P., Conte, V., Monte Carlo simulation of a new TEPC for microdosimetry at nanometric level: Response against a carbon ion beam. *Radiation Measurements*, 2018: 113: 7-13.
17. Bradley, P.D., Rosenfeld, A.B., Zaider, M., Solid state microdosimetry, *Nucl. Instrum. Methods*, 2001: B184, 135-157.
18. Agosteo, S., Pola, A., Silicon microdosimetry, *Radiation Protection Dosimetry* 2011:143: 409-415.
19. Rosenfeld, A. B., Novel detectors for silicon based microdosimetry, their concepts and applications. *Nuclear Instruments and Methods in Physics Research*, 2016: A809: 156-170.
20. Agosteo, S., Colautti, P., Fazzi, A., Moro, D., Pola, A., A solid state microdosimeter based on a monolithic silicon telescope. *Radiat Prot Dosimetry*, 2006: 122: 382-386.
21. Agosteo, S., Fallica, P.G., Fazzi, A., Introini, M.V., Pola A., and Valvo, G., A pixelated silicon telescope for solid state microdosimetry. *Radiation Measurements*, 2008: 43: 585-589.
22. Kellerer, A.M., Criteria for the equivalence of spherical and cylindrical proportional counters in microdosimetry. *Radiation Research*, 1981: 86: 277-286.
23. Agosteo, S., Cirrone, G.A.P., Colautti, P., Cuttone, G., D'Angelo, G., Fazzi, A., Introini, M.V., Moro, D., Pola, A., Varoli V., Study of a silicon telescope for solid state microdosimetry: preliminary measurements at the therapeutic proton beam line of CATANA. *Radiation Measurements*, 2010: 45: 1284-1289.
24. Colautti, P., Conte, V., Selva, A., Chiriotti, S., Pola, A., Bortot, D., Fazzi, A., Agosteo, S., Treccani, M., De Nardo, L., Verona, C., Verona Rinati, G., Magrin, G., Cirrone, G.A.P., Romano, F., Miniaturized microdosimeters as LET monitors: First comparison of calculated and experimental data performed at the 62 MeV/u <sup>12</sup>C beam of INFN-LNS with four different detectors. *Physica Medica*, 2018: 52: 113-121.
25. Colautti, P., Conte, V., Selva, A., Chiriotti, S., Pola, A., Bortot, D., Fazzi, A., Agosteo, S., Ciocca, M., Microdosimetric study at the CNAO active-scanning carbon-ion beam, *Radiation Protection Dosimetry*, 2018: 180: 157-161.
26. Bianchi, A., Selva, A., Colautti, P., Bortot, D., Mazzucconi, D., Pola, A., Agosteo, S., Petringa, G., Cirrone, G.A.P., Reniers, B., Parisi, A., Struelens, L., Vanhavere, F., Conte, V., Microdosimetry with a sealed mini-TEPC and a silicon telescope at a clinical proton SOBP of CATANA. *Radiation Physics and Chemistry*, 2020: 171: 108730.

